Single Side-Band Suppressed Carrier RF Processing

Sergio Granieri[1], Azad Siahmakoun[1], Steven Hughes and Bruce Black[2]
Rose-Hulman Institute of Technology,
Terre Haute, Indiana 47803

Jeff Chestnut and Dean Thelen
Naval Surface Warfare Center, Crane Division
Crane, Indiana 47522

ABSTRACT

We present a simple scheme for implementation of optical single sideband suppressed carrier (OSSB-SC) modulation based on the use of standard MZM and passive fiber optic components. The function of the proposed modulator is also theoretically predicted. A Sagnac interferometer structure is used for sideband suppression. The light propagating in one direction is orthogonally linearly polarized to the oppositely propagating light. The orthogonal polarization is implemented by a non-reciprocal optical element. The optical carrier is attenuated by appropriately setting the Mach-Zender Modulator (MZM) at quadrature bias point. We will experimentally demonstrate sideband suppression and carrier attenuation up to 28 dB by using all commercially available components.

Keywords: Single sideband suppressed-carrier modulation, Sagnac interferometer, RF modulation

1. INTRODUCTION

The advantages of single sideband (SSB) or single sideband suppressed carrier (SSB-SC) modulation, such as spectral power efficiency, have long been known in all electronic communication systems. The extension of the same techniques to optical communication can provide similar benefits, as well as new ones including mitigation of optical dispersion penalties.

In this paper we propose and experimentally demonstrate a direct implementation of a SSB-SC optical modulator using a using a commercial electro-optic Mach-Zender modulator (MZM) inside a fiber optic Sagnac interferometer. The suppression of the carrier is achieved by properly biasing the MZM in the lowest intensity transmission point, while the sideband is suppressed by placing a non-reciprocal phase shifter in the fiber interferometer.

In section 2 we describe in detail the theory for carrier suppression and SSB modulation. In section 3 the experimental setup is presented and discussed. In section 4 experimental results for carrier and sideband suppression from 0.1 GHz to 2 GHz modulation signals are presented together with the advantages and limitations of this approach. Concluding remarks are given in section 5.

2. THEORY

2.1 Carrier suppression with the Mach-Zender modulator

Consider an optical carrier signal out of one arm of the MZM is expressed as

$$E = E_0 \exp\left(i w_c t + \frac{i p V_t}{2 V_p} \right) \tag{1}$$

$$V_t = V_0 + V_m \sin(w_m t) \tag{2}$$

In these equations ω_c is the carrier or laser frequency, V_m is the modulation voltage, V_0 the DC bias, and V_π is the voltage necessary for a π phase shift in the intensity output of the MZM. Since there are two arms in the MZM path 1 is the wave traveling in one arm while path 2 is the wave traveling in the other arm, both of which are in the form of (1). Adding path 1 to 2, which differ by only a phase difference arising from a $-V_t$ as in Ref.1, the output signal consists of an non modulated

[1] Author are with the Department of Physics and Applied Optics
[2] The author is with the Department of Electrical and Computer Engineering

signal at the carrier frequency and an RF signal in the sidebands arising from (2). As the RF frequency (ω_m)is modulated the sideband frequency is modulated as well.

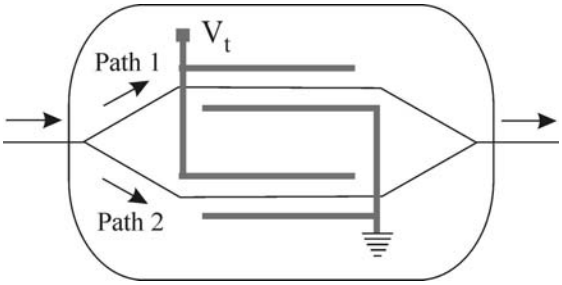

Fig.1: Schematic of light paths through MZM

Most applications only desire the signal in the sidebands, which carry the optical signal. The carrier just consumes power from any amplifier and thus would ideally be eliminated leaving just the sidebands. The output of the MZM converted from exponentials to sinusoids results in:

$$E_{mzm} = \frac{1}{2}\cos(w_c t)\cos\left(\frac{p\,V_0}{2V_p}\right)\cos\left(\frac{p\,V_m\cos(w_m t)}{2V_p}\right) - \frac{1}{2}\cos(w_c t)\cos\left(\frac{p\,V_0}{2V_p}\right)\sin\left(\frac{p\,V_m\cos(w_m t)}{2V_p}\right) \tag{3}$$

To actually view the frequency components from Eq. (3) take its Bessel expansion, which will yield;

$$\begin{aligned} E_{mzm} = {} & \frac{1}{2}\cos(w_c t)\cos\left(\frac{p\,V_0}{2V_p}\right)\left\{J_0\left(\frac{p\,V_m}{2V_p}\right) + 2\left[\sum_{n=1}^{N}(-1)^n J_{2n}\left(\frac{p\,V_m}{2V_p}\right)\cos(2n w_m t)\right]\right\} - \\ & - \cos(w_c t)\sin\left(\frac{p\,V_0}{2V_p}\right)\left[\sum_{n=1}^{N}(-1)^n J_{2n+1}\left(\frac{p\,V_m}{2V_p}\right)\cos((2n+1)w_m t)\right] \end{aligned} \tag{4}$$

By setting the bias voltage of the MZM $V_0=V_\pi$, the carrier term and even sidebands go to zero leaving only the odd sidebands. Therefore with the MZM alone we can cancel the carrier leaving the Sagnac, by adjusting the relative phase of the counter-propagating field, to cancel the sideband yielding;

$$E_{sag} = \sum_{n=1}^{N}\left[\frac{1}{2}(-1)^n J_{2n+1}\left(\frac{p\,V_m}{2V_p}\right)\cos[(w_c + (2n+1)w_m)t] + \frac{1}{2}(-1)^n J_{2n+1}\left(\frac{p\,V_m}{2V_p}\right)\cos[(w_c - (2n+1)w_m)t]\right] \tag{5}$$

From Eq. (5) one can easily see the surviving frequencies occur at $\omega_c\pm\omega_m$, $\omega_c\pm 3\ \omega_m$, $\omega_c\pm 5\ \omega_m$...

2.2 Sideband suppression

Ideally, the polarized light entering the pigtailed beam splitter is split 50/50 into two arms, which when connected together make the Sagnac. The light traveling in both directions will be in the transmission axis of the PM fiber through the loop and have the basic equation for each direction.

$$E = E_0 \cdot \exp\left(i w_c t + \frac{ip V_t}{2V_p} + f_{BS} + f_{NRPS}\right) \tag{6}$$

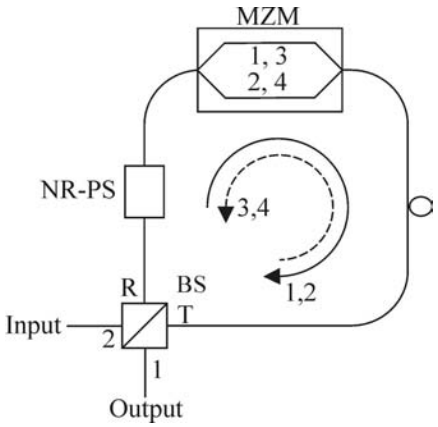

Fig. 2: Schematic of the Sagnac interferometer. Numbers 1,2,3 and 4 are different paths through the MZM.

ϕ_{NRPS} is the phase delay for paths 1&2 through the NRPS with respect to paths, 3&4 which travel in the opposite direction through the Sagnac. The NRPS, is introduced in the form of a quarter waveplate between two faraday rotators, within the Sagnac. This element allows for the $\pi/2$ optical carrier phase shift necessary for sideband cancellation.

Another non-reciprocal phase shift is introduced due to the beam splitter in the Sagnac causing one path to be reflected twice and the other to be transmitted twice. The ϕ_{BS} is this phase difference with the same effects as the NRPS but must be solved for experimentally and can be included in the NRPS variable. Simplifying an equation in the form of (5) and inserting the value of $\pi/2$ for ϕ_{NRPS} gives:

$$\begin{aligned} E = &\sum_{n=0}^{N}\left[-\frac{1}{2}(-1)^n J_{2n+1}\left(\frac{p\,V_m}{2V_p}\right)\cos\left[\left(w_c+(2n+1)w_m\right)t\right]\right]+ \\ &+\sum_{n=0}^{N}\left[-\frac{1}{2}(-1)^n J_{2n+1}\left(\frac{p\,V_m}{2V_p}\right)\cos\left[\left(-w_c+(2n+1)w_m\right)t\right]\right]+ \\ &+\sum_{n=0}^{N}\left[\frac{1}{2}(-1)^n J_{2n+1}\left(\frac{p\,V_m}{2V_p}\right)\cos\left[\left(w_c+(2n+1)w_m\right)t\right]\right]+ \\ &+\sum_{n=0}^{N}\left[-\frac{1}{2}(-1)^n J_{2n+1}\left(\frac{p\,V_m}{2V_p}\right)\cos\left[\left(-w_c+(2n+1)w_m\right)t\right]\right] \end{aligned} \tag{7}$$

From this it can easily be seen that only every other odd sideband survives in the form of $\omega_c+\omega_m$, $\omega_c-3.\omega_m$, $\omega_c+5.\omega_m$

3. EXPERIMENTAL SETUP

3.1 System

A Santec ECL-200 tunable Laser Diode (LD) source at 1550nm launches into a Polarization Maintaining (PM) fiber, which is immediately polarized with a pigtailed polarizer to ensure propagation only within the transmission axis. To suppress the sideband a fiber optic Sagnac interferometer is setup with the MZM inside as shown in Figure 3.

The beam is then split though a pigtailed PM BS. The outputs of both the R-port and T-port make up the two inputs of the Sagnac. The T-port pigtail is immediately connected to a JDS Uniphase MZM and then to the first PM pigtailed Faraday rotator of the NRPS. The output of this rotator is routed through an OZ Optics PM pigtailed quarter waveplate and through the second rotator back to the R-port of the BS. The MZM is not symmetrically placed in the Sagnac with respect to the BS giving rise to a $\Delta\tau$ time difference for the RF modulation as the optical carrier recombines at the BS [2].

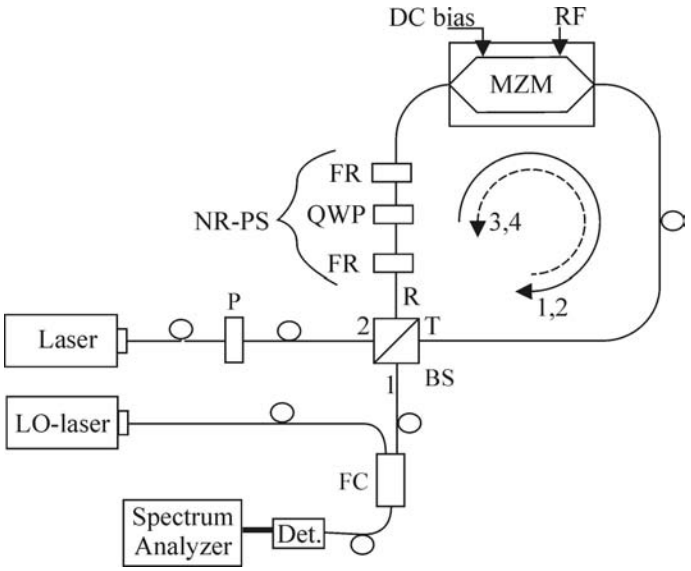

Fig.3: Experimental setup: BS: Beam splitter, FC: Fiber coupler, P: Polarizer, FR: Faraday Rotator, QWP: Quarter-Wave plate

The BS transmits 36.26 and 34.95% to its R and T ports respectively which have pigtails 1.10m long. In its off state the MZM experiences a 7.34 dB and a 8.16 dB loss though its forward and reverse directions respectively. The faraday rotators have pigtails on both ends of length 1.10 m. The total asymmetric length resulting in $\Delta\tau$ is 6.59m. The quarter waveplate's loss varies with the orientation of the waveplate axis to the fiber slow axis, and has pigtails 1.15 m long. To attain a readable signal a Local Oscillator is beat against the output of the Sagnac to generate a signal the detector can pick up. The output of the Sagnac with the LO is converted to an electric signal with a Discovery Semiconductor InGaAs DSC20S detector, which is read by a Tektronix 2782 Spectrum Analyzer. The RF input is generated by an HP 83650A Synthesized Sweeper and is varied from 100MHz to 2GHz.

3.2 Polarization maintaining fiber and Faraday rotators

The pigtails and fiber links between all components are comprised of birefringent polarization maintaining fiber. This fiber ensures that light launched into the transmission axis will stay polarized in that axis when it exits the fiber regardless of length. The only point at which the light can change between fast and slow axis of the fiber is in the faraday rotator or in the MZM which is not made with PM fiber.

The faraday rotators are set to 45^0 rotation and thus the transmission axis after the rotator is also offset by 45^0. This ensures that light traveling through the rotator in the forward direction stays in the transmission axis, but light traveling in reverse is shifted into the second axis as in the figure below.

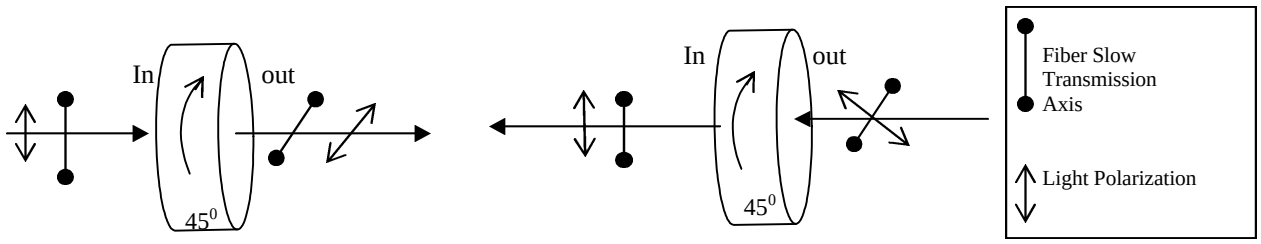

Fig. 4: Pigtailed Faraday rotators with left: forward and right: reverse propagation of polarized light

In this diagram the transmission axis is shown rotated 45° on the out side of the rotator. The *right* diagram shows light traveling in the fast axis being rotated into the slow axis, though if it were in the slow axis initially it would be coupled to

the fast axis. Likewise the lift diagram shows that in the forward direction light will be coupled into the same axis it originated from, fast or slow.

3.3 Non-reciprocal phase shifter

By placing two of these rotators in series (In-out: In-out) there will be a segment of the fiber between them in which the light in one direction will be in the slow axis while the other propagates in the fast. This allows for a NRPS to occur in this segment of fiber. Varying the length of the fiber between the rotators, or placing a waveplate between them allows for further control over the phase shift.

Additional configurations can be made by changing to (In-out ; out-In) and by placing a 90^0 coupler between or on one end of the series of rotators. Unfortunately, due to the length of the pigtails, thermal fluctuations can change the length of the birefrengent fiber thus varying the phase difference between the two directions. For this reason it is ideal to keep the Non-Reciprocal segment between the rotators and to keep this length as short as possible.

3.4 Beat with a local oscillator

Due to the high frequency of the carrier, 193.5 THz, the output of the Sagnac is beat against a local oscillator laser referenced at a frequency displaced by 3GHz [3]. This allows our Tektronix spectrum analyzer model 2782 to display the necessary carrier and its sidebands. The frequency of the beating can be found with the equation $\delta_\nu = c.\delta_\lambda/\lambda^2$, which for our case was .024 nm yielding approximately 3GHz beating.

4. RESULTS

Since the beam splitter causes one path to be reflected twice and the other to be transmitted twice a 8π / 9 phase difference is generated. This shift can only be adjusted to the required 90° with NRPS that is why the two values are combined in one variable. Were one to be adjusted the other value can be compensated yielding the same output. Either the asymmetry of the MZM or the NRPS can be compensated to attain maximum modulation efficiency, though neither is easy to adjust. Due to the pigtails we can only look for specific frequencies at which the asymmetry of the MZM will allow sideband suppression. Equation (9) shows the necessary condition for sideband suppression of the n^{th} sideband.

$$\frac{p}{2} + 2p\ n = 2p\ \frac{n\ n\ \Delta L}{c} \tag{9}$$

In this equation ν is the RF frequency and ΔL is the path difference due to the asymmetric placement of the MZM. To suppress the opposite n^{th} band replace the $\pi/2$ with $3\pi/2$. Because we cannot adjust the path length of the fibers, data taken for around 100MHz is actually taken at frequencies at which the path length contributes to the necessary phase shift to attain sideband suppression as in Fig 4 or only carrier suppression in Fig 3.

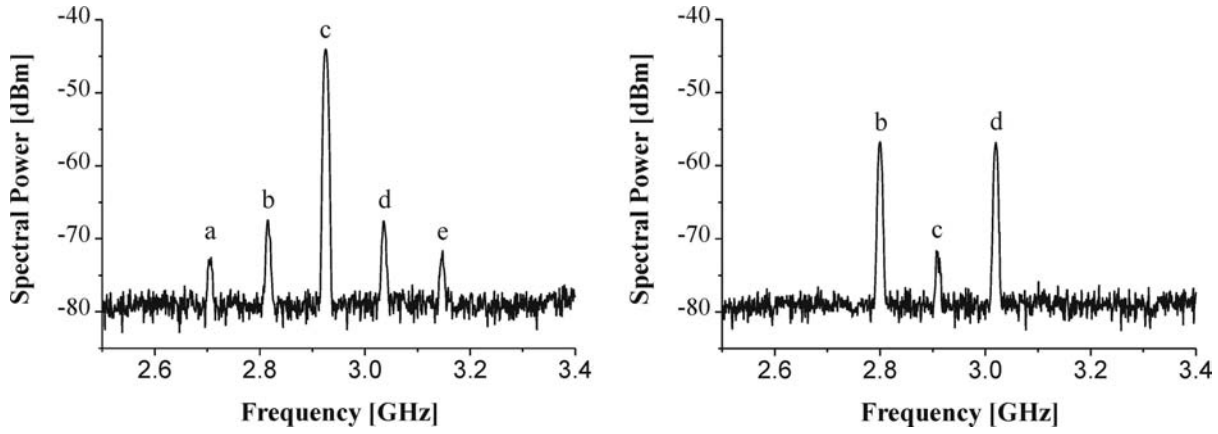

Fig. 5: Left: unsuppressed carrier (USC), Right: suppressed carrier (SC) causing sideband amplification of b and d while suppressing a and e. Modulation voltage is 16dBm. C is the carrier, b and d the first order sidebands, and a and e the 2^{nd} order sidebands.

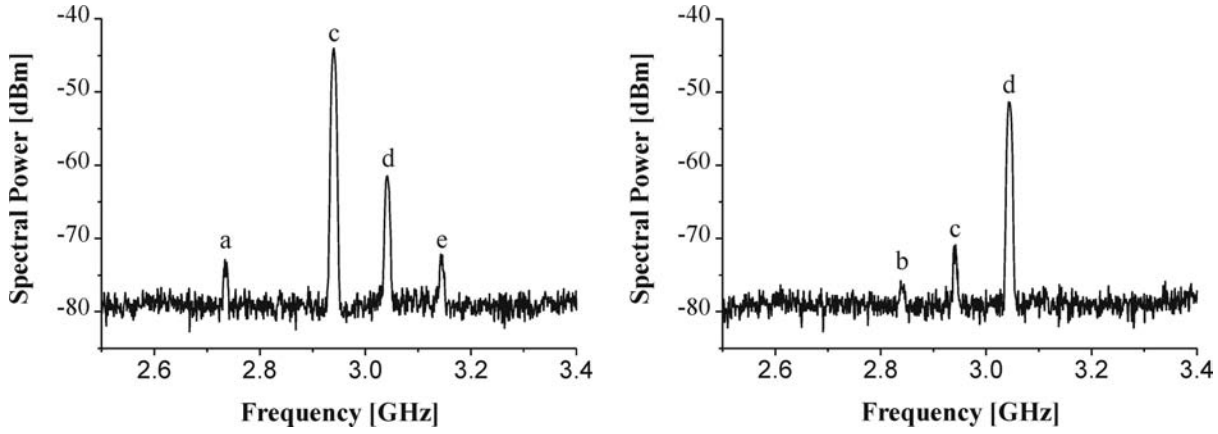

Fig. 6: Left: b is suppressed, Right: b is suppressed still but suppressing c also suppresses a and e. Modulation voltage is 16dBm

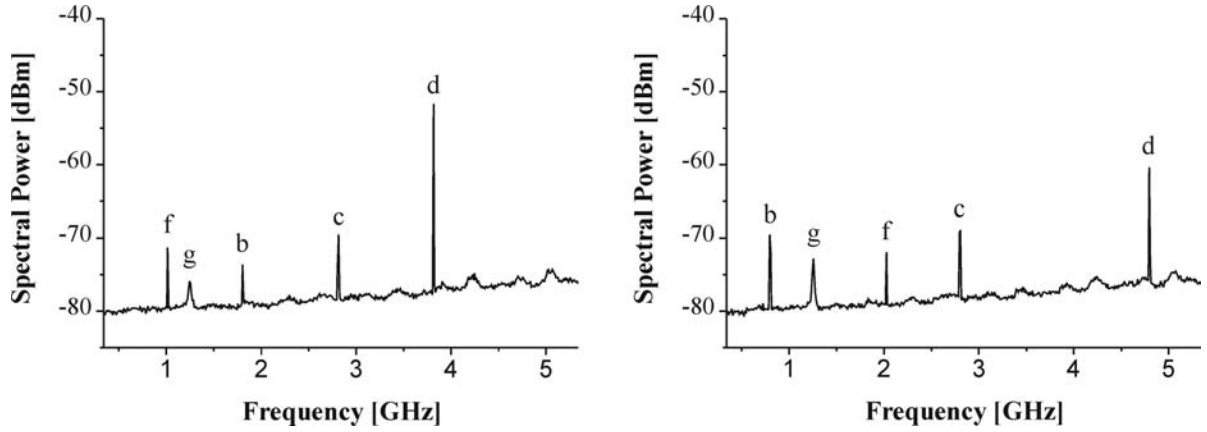

Fig. 7: These are exactly the same as Fig. 4 right except due to higher frequencies suppression is less efficient and there are two new peaks, f: the RF frequency and g: an artifact of the spectrum analyzer.

Lower sideband data is essentially symmetric about the carrier and thus are not shown. The Carrier in all of these plots is at approximately 3GHz. For higher RF frequencies both interferometers become less effective at suppressing the carrier and sidebands, which results in a decreased suppression as shown below.

While the RF changing does not significantly affect the V-bias needed to cancel the carrier in the MZM, the RF phase shift will only cancel certain integer multiple frequencies thus decreasing suppression efficiency for larger deviations in RF frequency. Additionally, due to the NRPS if the DC bias is not applied thermal fluctuations in the non-reciprocal arm of the system causes greater instability in the carrier amplitude.

One of the important characteristics of this setup is the amount of deviation from these certain frequencies that will still adequately suppress the sideband to maintain 20dB difference between the desired sideband and the other frequency components. Suppression is achieved for both the carrier and sideband up to 25 dB below the remaining sideband though the intensity is only roughly 30dB above the noise floor. Losses in the system are considerable, especially at the quarter waveplate and polarizer yielding a power output below –8dBm. Incomplete carrier suppression can be attributed to imprecise DC bias on the MZM which results in a deviation from the necessary $\pi/2$ shift between the arms of the MZM, which can cause relatively large deviations, 10dB or more, above complete carrier suppression. Also, different modulation efficiencies in one arm of the MZM vs. the other, or unequal splitting of light between the arms would cause incomplete

carrier suppression. If the NRPS or MZM has problems as mentioned above, then changes in the RF frequency will also contribute.

Incomplete sideband suppression can also be attributed to a possible Doppler shift in interaction between the modulation frequency wave and the carrier. This may occur since our MZM only modulates with the applied field traveling in one direction before dropping potential across a 50 Ω load, though it is unlikely this plays a significant role. Another cause for incomplete carrier suppression can be imperfections in the 50/50 splitter ratio. In both cases the amplitude of the suppressed sideband is constant and does not change when the carrier is suppressed.

Calculations show that the raising of the suppressed sideband through suppression of the carrier can be caused by the imperfections in the NRPS, the asymmetrical placement of the MZM, or the asymmetrical modulation and losses of the MZM. When suppressing the carrier, imperfections in any one of these contribute to the increase in amplitude of the suppressed sideband as well as the desired sideband, which should experience the amplification. Additionally, should the deviation of the NRPS or the placement of the MZM be equal and opposite to the deviation of the other, complete sideband suppression will occur. However, under this condition, larger deviations from $\pi/2$ will cause the amplitude of all peaks to decrease uniformly. This may allow active compensation to keep the sideband suppressed, especially for thermal fluctuations causing shifts in either element, though it would only be recommended for small compensation. A Temperature controller or piezo crystal device to change the path length should help with this problem.

It was also noted that a 10-degree misalignment in one of the faraday rotators would hinder complete suppression of the sideband. This misalignment would cause a portion of light to propagate in the wrong axis of the fiber resulting in a component out of the Sagnac, which is improperly suppressed.

5. CONCLUSIONS

For frequencies of 1GHz and under, at least with the JDS Uniphase MZM, this system delivers a single sideband 20dB or more above the other bands. This would allow for amplification of the signal with an EDFA or some other means without wasting much of the gain on useless information in the carrier or other peaks. To improve on this design the faraday rotators need to be placed adjacent to the waveplate, which should improve stability of suppression. It is likely that by fixing this and adding the EOM in place of the waveplate that the system can be adjusted for any RF rather than having to use certain calculated modulation frequencies.

ACKNOWLEDGMENTS

The authors would like to thank Dan Purdy of Office of Naval Research for his support of this project under the contract number N00014-00-1-0782.

REFERENCES

1. R. Montgomery, and R. DeSalvo, "A Novel Technique for Double Sideband Suppressed Carrier Modulation of Optical Fields*," IEEE Photonics Technol. Lett*., **7**, pp. 434-436, 1995.

2. A.Loayssa, J.M. Salvide, D. Benito and M.J. Garde, "Novel Optical Single-Sideband Suppressed-Carrier Modulator Using Bidirectionally-Driven Electro-optic Modulator", *Technical Digest: Microwave Photonics 2000 conference,* Alwyn Seeds, pp.117-120, IEE, Oxford, 2000.

3. M.Y. Frankel, and R.D. Esman, "Optical Single-Sideband Suppressed-Carrier Modulation for Wide-Band Signal Processing," *J. of Lightwave Technol*., **16,** pp. 859-862,1998.